Gas Phase Absorption Studies of Photoactive Yellow Protein Chromophore Derivatives

Tomás Rocha-Rinza,[†] Ove Christiansen,[†] Jyoti Rajput,[‡] Aravind Gopalan,[‡] Dennis B. Rahbek,[‡] Lars H. Andersen,*[,‡] Anastasia V. Bochenkova,[¶] Alexander A. Granovsky,[¶] Ksenia B. Bravaya,[¶] Alexander V. Nemukhin,[¶] Kasper Lincke Christiansen,[§] and Mogens Brøndsted Nielsen[§]

Lundbeck Foundation Center for Theoretical Chemistry and Center for Oxygen Microscopy and Imaging (COMI), Department of Chemistry, University of Aarhus, DK-8000 Aarhus C, Denmark, Department of Physics and Astronomy, University of Aarhus, DK-8000 Aarhus C, Denmark, Department of Chemistry, M.V. Lomonosov Moscow State University, Moscow 119991, Russia, and Department of Chemistry, University of Copenhagen, DK-2100 Copenhagen Ø, Denmark

Received: May 26, 2009; Revised Manuscript Received: June 26, 2009

Photoabsorption spectra of deprotonated *trans p*-coumaric acid and two of its methyl substituted derivatives have been studied in gas phase both experimentally and theoretically. We have focused on the spectroscopic effect of the location of the two possible deprotonation sites on the *trans p*-coumaric acid which originate to either a phenoxide or a carboxylate. Surprisingly, the three chromophores were found to have the same absorption maximum at 430 nm, in spite of having different deprotonation positions. However, the absorption of the chromophore in polar solution is substantially different for the distinct deprotonation locations. We also report on the time scales and pathways of relaxation after photoexcitation for the three photoactive yellow protein chromophore derivatives. As a result of these experiments, we could detect the phenoxide isomer within the deprotonated *trans p*-coumaric acid in gas phase; however, the occurrence of the carboxylate is uncertain. Several computational methods were used simultaneously to provide insights and assistance in the interpretation of our experimental results. The calculated excitation energies S_0-S_1 are in good agreement with experiment for those systems having a negative charge on a phenoxide moiety. Although our augmented multiconfigurational quasidegenerate perturbation theory calculations agree with experiment in the description of the absorption spectrum of anions with a carboxylate functional group, there are some puzzling disagreements between experiment and some calculational methods in the description of these systems.

Introduction

Light is perceived by a vast majority of living organisms, and it drives many important chemical and biological phenomena of which photosynthesis and vision are perhaps the two most prominent examples. However, light may also induce a wide variety of other biological responses. Phototaxis, the movement of an organism as a consequence of its exposure to light, is another photochemical functionality which is biologically relevant. For instance, bacteria can move either toward more strongly illuminated areas (positive phototaxis) to receive light for photosynthesis[1,2] or to regions with less intensity of radiation (negative phototaxis)[2] to escape from potentially harmful light.

The photoactive center in all such biological systems is a light absorbing molecule (chromophore) enclosed within a protein. The photoactive yellow protein (PYP) is the photoreceptor responsible for the negative phototaxis of its host[3] and has become a standard model in photochemistry and photobiology[4] leading to a considerable amount of experimental[3−10] and theoretical[11−16] studies. PYP encompasses the chromophore *trans p*-coumaric acid (pCA) which is covalently linked to the protein via a thioester bond to cysteine 69 and triggers photomovement by absorbing blue light.[5] In the ground state, the chromophore is an anion (pCA^-) in the trans form. This allows the stabilization by hydrogen bonds from two neighboring amino acids, Glu46 and Tyr42[8,17] as can be seen in Figure 1. The pCA^- chromophore is also stabilized by cation-π and π-stacking interactions with Arg52 and Phe96 respectively.

The spectroscopic properties of pCA^- are fundamental for the biological signaling of PYP. Measurements done in the absence of protein interactions are of great importance because they serve to test the intrinsic characteristics of the chromophore and to assess theoretical efforts in describing the properties of photoactive proteins. Earlier gas-phase photoabsorption studies upon pCA^- anions generated with an electrospray-ionization technique have shown that the previously described protein environment does not shift the absorption maximum of the chromophore by a signicant amount while the aqueous environment induces a large blue shift, especially in neutral and low values of pH.[18] Nonetheless, because pCA has two acidic protons, its gas-phase structure produced by the electrospray technique is unclear.[19] The two possible isomers of pCA^-, a carboxylate or a phenoxide (Figure 2A), are expected to have different absorption properties. Therefore, we measured the absorption spectrum of pCA^- along with those of two of its methyl derivatives (Figure 2B,C) in an attempt to determine its gas-phase structure and to clarify the role of the deprotonation site of the chromophore on its spectral response. The methyl substituted derivatives have only one acidic proton, and the use of these systems allows the absorption of the phenoxide and the carboxylate form of the chromophore to be studied

* Corresponding author. E-mail: lha@phys.au.dk.
[†] Department of Chemistry, University of Aarhus.
[‡] Department of Physics and Astronomy, University of Aarhus.
[¶] M.V. Lomonosov Moscow State University.
[§] University of Copenhagen.

10.1021/jp904660w CCC: $40.75
Published on Web 07/30/2009

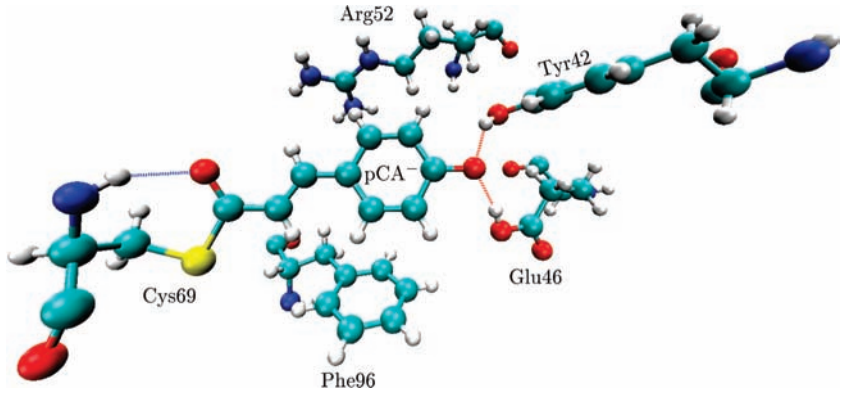

Figure 1. Deprotonated *trans p*-coumaric acid (pCA^-) and its neighboring environment within the photoactive yellow protein in its ground state.

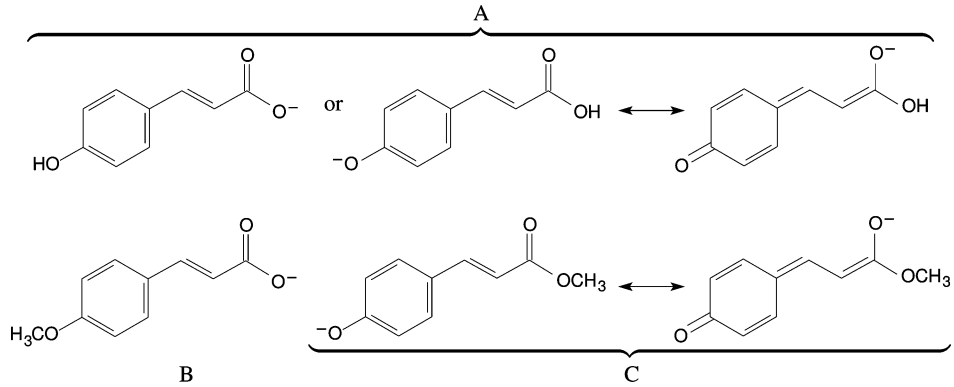

Figure 2. Chromophores addressed in this work: **A** is the deprotonated *trans p*-coumaric acid in the form of either a carboxylate (left) or a phenoxide (right) while **B** and **C** are the corresponding derivatized methyl ether and ester respectively.

separately. We also compared the decay modes of the chromophores which show photodissociation as a mode of relaxation after photoexcitation in the gas phase. The complex dynamics associated with the photodissociation pathways of pCA^- had been previously shown to include fragmentation and electron detachment[20] as photoresponse processes. Finally, we also carried out theoretical calculations aimed to complement and provide assistance to the interpretation of our experimental results.

Experimental and Computational Methodologies

The chromophores *trans p*-coumaric acid and its methoxy derivative *trans p*-$CH_3OC_6H_4-CHCH-COOH$ were purchased from Aldrich. The methyl ester derivative *trans p*-$HOC_6H_4-CHCH-COOCH_3$ was prepared according to a literature procedure.[21] The gas-phase absorption spectra were recorded at the electrostatic storage ring ELISA.[22] The technique of daughter mass analysis[23] was used to determine the mass of possible fragments that may be generated after laser excitations. Finally, the fast dissociation dynamics of the systems presenting prompt channels at ELISA were studied at a linear time-of-flight (TOF) spectrometer with submicrosecond time resolution.[24,25]

The ground state geometries of all systems considered in this work were optimized using the hybrid B3LYP[26,27] and PBE0[28] functionals and the correlation-consistent basis set augmented with diffuse functions aug-cc-pVDZ.[29,30] Every stationary point of the potential energy surface was confirmed to be a local minimum by calculating the vibrational frequencies at the same level of theory. Vertical excitation energies were calculated with five different approximations. More precisely, we used the black box ground state linear response methods: (i) the approximate coupled cluster singles and doubles CC2[31] in its efficient resolution of the identity variant[32,33] (RI-CC2) and (ii) time-dependent density functional theory (TDDFT) using the functional CAM-B3LYP.[34] In addition, the CASSCF[35] based perturbation theory approaches (iii) the state-specific MRMP2,[36] (iv) its multistate extension MCQDPT2,[37] and (v) the augmented version of the multiconfigurational quasidegenerate perturbation theory aug-MCQDPT2[38] were utilized. We used the basis set (p type) d-aug-cc-pVDZ[29,30] (i.e., the only considered functions from the spd shell of diffuse functions are of p type) along with the multireference perturbation theory methods, MRMP2, MRMP2 and aug-MCQDPT2. The linear response methods, RI-CC2 and CAM-B3LYP, were applied with the aug-cc-pVTZ[29,30] basis set. Additional calculations of the n-π^* vertical excitation energies and ionization potential thresholds from n and π orbitals were also carried out at the RI-CC2/aug-cc-pVTZ and MRMP2/aug-cc-pVTZ levels in the case of system B. Further details about the experimental procedures and the carried out calculations can be found in the Supporting Information.

Results and Discussion

Absorption Spectra. The gas phase absorption spectra of the three model chromophores are shown in Figure 3. Surprisingly, all three chromophores show an absorption maximum at 430 ± 3 nm. In addition, a small structure just below 400 nm is observed for samples B and C.

In principle, there may exist two forms of system A, each originating from the two different deprotonation sites of pCA. Since carboxylic acids, in general, have larger acidity constants than phenols, chemical common sense indicates that the structure of pCA^- in solution is a carboxylate rather than a phenoxide.

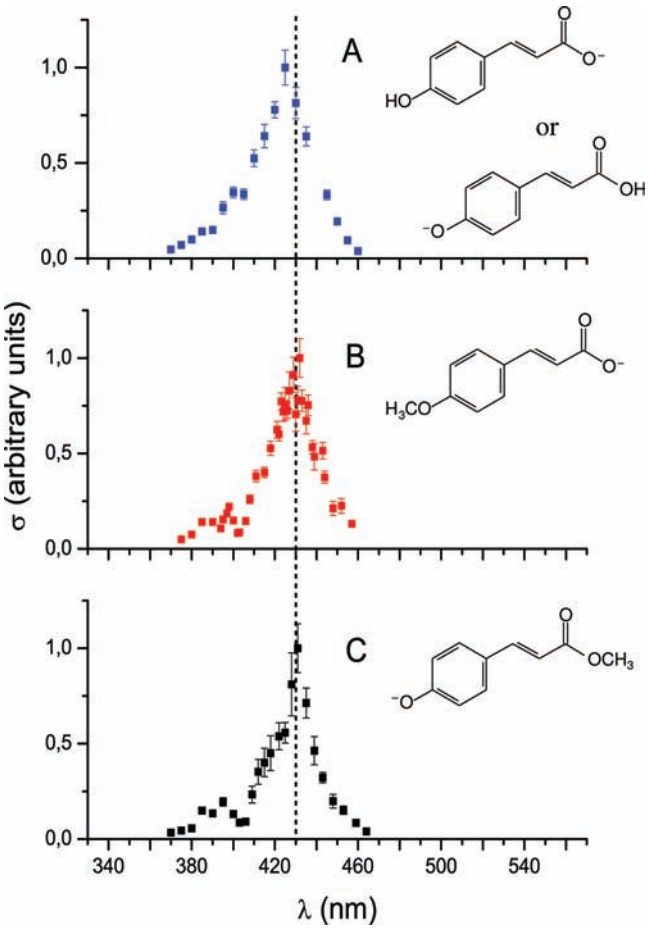

Figure 3. Absorption spectra of the photoactive yellow protein chromophore models in gas phase addressed in this work. The maxima are known with an uncertainty of 3 nm.

Indeed, the two pK_a values in aqueous solution of pCA, 4.360 ± 0.003 and 8.982 ± 0.001,[39] are typical of a carboxylic acid and a substituted phenol with a moderate electron-withdrawing group in para position,[40] respectively. However, the relative acidity of the phenolic and carboxylic protons may be reversed in the gas phase. The phenoxide form of pCA^- is 13 kcal/mol more stable than the carboxylate at the DFT and RI-CC2 approximations. This can be rationalized in terms of the negative charge stabilization depicted by the two resonance structures which span the entire conjugated π-system in Figure 2A. The importance of the quinone-like resonance structure for the phenoxide is reflected in the reduction of the bond lengths O(1)−C(1), C(2)−C(3), C(5)−C(6), C(4)−C(7), and C(8)−C(9) with respect to the carboxylate as shown in Figure 4. The rest of the bond lengths in the π system exhibit the opposite behavior. Although the phenoxide structure is energetically more favorable in the gas phase, it is possible that the applied electrospray-ionization technique using solvated chromophore ions as a starting point favored the kinetically controlled product, that is, the carboxylate due to the likely pronounced energy barrier for the proton transfer in the gas phase.

Figure 3 shows that the substitution of a methyl group in place of an acidic hydrogen atom in pCA^- does not alter the energy gap between the ground and the first excited state. Because of the very similar absorption spectra of B and C, the role of the solvent in the interconversion of these systems was investigated. Such isomerization reactions were ruled out by mass analyses of ions, having as starting points the chromophores dissolved separately in CH_3CH_2OH. The interconversion of the functional groups of B and C in this solvent would have produced anions with a mass/charge ratio of 191 that is p-$CH_3CH_2OC_6H_4CHCH-COO^-$ or p-$^-OC_6H_4CHCHCOOCH_2CH_3$ which were not observed.

The equivalence of the spectra of the species A, B, and C indicates that the absorption of pCA^- occurs at the same wavelength in the gas phase regardless of its structure being a carboxylate or a phenoxide. However, the carboxylate B and phenoxide C absorb at different wavelengths in polar solutions. The absorption spectra of B and C in CH_3OH are shown in Figure 5 with the corresponding values of λ_{max} of 282 and 356 nm, respectively. It is known that the phenoxide and the phenol moieties exhibit different absorption maxima in protic solvents,[41] the former being red-shifted with respect to the latter, and one might be tempted to ascribe this fact as the main reason for the difference between the absorption spectra of B and that of C in methanol. However, the comparison between the two spectra should be done taking into account the entire π system of pCA^- in their carboxylate and phenoxide forms, because the carbonyl functional group affects the electronic properties of the phenolic oxygen and vice versa. The spectra in Figure 3 and that in Figure 5 imply that solvation by methanol results in a blue shift for both systems with a major effect for B. The difference in the absorption shift is due to the stronger interactions of B in comparison to those of C with polar hydrogen bonding solvents. The localized negative charge of the carboxylate group in B is more effectively stabilized by the polar solvent molecules than the delocalized charge in C. Besides, the transference of para-disubstituted benzene derivatives from an apolar environment to protic solvents is an enthalpically unfavorable process;[42] that is, the p-C_6H_4 group hinders the solvation of the phenolic oxygen by methanol, and esters are less soluble in H-bond solvents than carboxylic acids with a similar molecular weight.[43] The less efficient solvation of the phenolic oxygen in system C in comparison to the carboxylate group of system B is also evidenced by the fact that the phenoxide form of pCA^- is more stable than the carboxylate anion in gas phase, but still the latter isomer is the occurrent species in neutral values of pH in aqueous and alcoholic solution. In short, neither the phenoxide moeity nor the ester group of C can be as efficaciously solvated as the carboxylate group of B in CH_3OH. These effects induce a larger ground state stabilization by the alcoholic solvent for B as compared to C. Therefore, a larger blue shift in the absorption for system B with respect to gas phase is observed. The value of λ_{max} = 282 nm for B is very similar to the absorption maximum of pCA^- in neutral aqueous solution (λ_{max} = 285 nm)[18] in virtue of the carboxylate character of the two species and the resemblance of the interactions in both solvents. Still, it is worth noticing that the blue shift of B in polar solution is very large, and such effect should attract further theoretical and experimental research.

The calculated spectra at the RI-CC2 and CAM-B3LYP approximations are shown in Figure 6, and the results from the multireference perturbation theories MRMP2, MRMP2 and aug-MCQDPT2 are presented in Table 1. The functional CAM-B3LYP and the RI-CC2 method give a similar description of the electronic spectrum. It is observed, however, that some bands at one level of theory are split in the other. The strongest bands at 3.10 eV (400 nm) for RI-CC2 and 3.40 eV (365 nm) for CAM-B3LYP in the spectra of pCA^- in the form of phenoxide and of system C correspond to the absorption maximum at 430 nm displayed in Figure 3. The phenoxide anion of pCA is a case where the CASSCF description is good enough to get satisfactory results by conventional MRPT2 procedures. In this

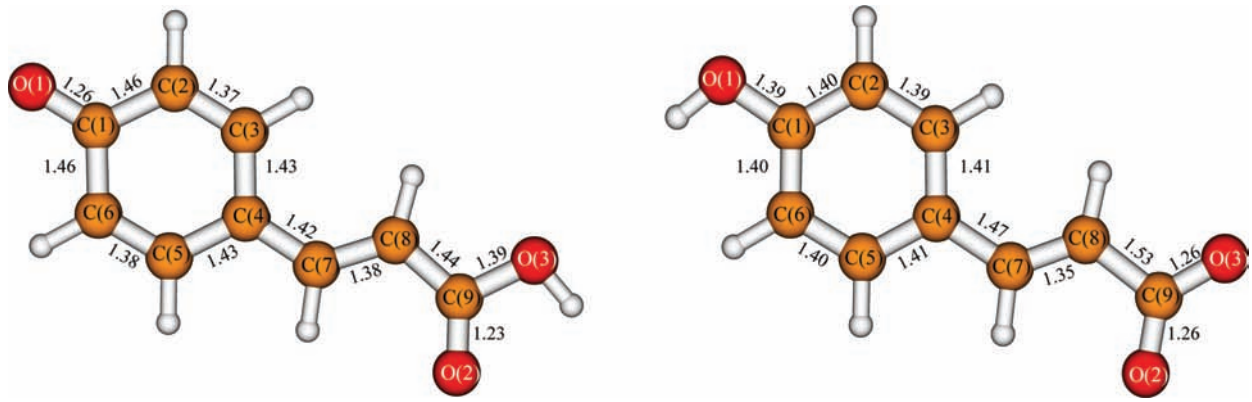

Figure 4. Bond lengths in Å within the π system in the phenoxide (left) and carboxylate (right) anions of *trans p*-coumaric acid. The comparison shows that the quinone-like resonance structure of Figure 2C is more important for the former than for the latter.

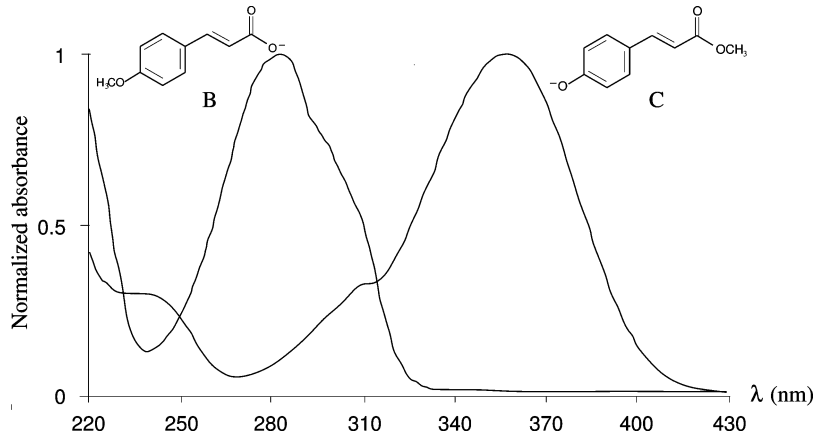

Figure 5. Normalized absorption spectra in CH_3OH of species **B** and **C** with absorption maxima at 282 and 356 nm respectively. Spectra were obtained by dissolving the neutral precursors in CH_3OH with subsequent addition of $NaOCH_3$.

case, the negative charge is effectively delocalized along the π-conjugated system; the target $\pi-\pi^*$ excited state is dominated by the single one-electron excitation affecting the negative charge. The S_0-S_1 excitation wavelength obtained with the state-specific MRMP2 methodology, 444 nm, can be compared to those calculated by the multistate MCQDPT2 approximation with a small and an enlarged dimension of the effective Hamiltonian, 441 and 440 nm respectively, and with the approximations RI-CC2, 400 nm, and CAM-B3LYP, 365 nm, as can be read in the last column of Table 1. Still, it is clear that the linear response methodologies do not have a good agreement with experiment for the systems having the negative charge on a $-COO^-$ group. Neither the phenoxide nor the carboxylate anions are expected to have a multiconfigurational character in the ground state. In addition, none of the parameters testing the quality of the linear response results indicated an important double-excitation character in the electronic excitation of the carboxylates which would degrade the accuracy of the calculations. In addition, the exploratory computation of the excitation energies employing up to triple excitations in coupled cluster theory did not give indications of such problems. This makes it complicated to explain the discrepancy of RI-CC2 and CAM-B3LYP results relative to experiment.

It is worth noting that the calculated energies of the most intensive transitions which can be assigned to the experimental absorption maxima of the carboxylate anions of systems A and B are overestimated compared with experiment but remarkably close to each other within the CAM-B3LYP, RI-CC2 and state-specific MRMP2 approximations as seen in Table 1. Moreover, the MRMP2/CASSCF and RI-CC2 methodologies predict a qualitatively similar spectrum of the carboxylate form of system A, despite the large differences in the approaches of these methods. Low-lying charge transfer transitions with very low intensity were found, while the bright target excited state appeared to be relatively high in energy as shown in Table 2. The agreement between MRMP2 and RI-CC2 and the disagreement of the linear response methods RI-CC2 and CAM-B3LYP with experiment are baffling. In this regard, the MRMP2 description of the carboxylate form of pCA^- is discussed further below.

A reasonably good account at the CASSCF level is a prerequisite for the successful application of MRMP2. In this regard, system A in the form of carboxylate is a particular case of a highly insufficient CASSCF description of the first excited state because of the lack of dynamic electron correlation. An overestimation of the role of charge transfer excitations related to the redistribution of electron density of the carboxylate group along the conjugated π-system gives a poor characterization of low-energy excited states at the CASSCF level. The target valence excited state, dominated by a single-electron excitation in the central part, does not affect the negative charge explicitly and turns out to be fairly high in energy because of the electrostatic repulsion of the localized carboxylate charge and the diffuse electron density of the rest of the molecule. This target excitation correlates with the HOMO$-$LUMO transition. The state-specific MRPT2 cannot even improve the ordering of the states. The target excited state is the sixth root at the CASSCF and MRMP2 levels. An incorrect ordering leads also to the coupling of the states erroneously lying close in energy. The target state of the carboxylate anion of system A is mixed

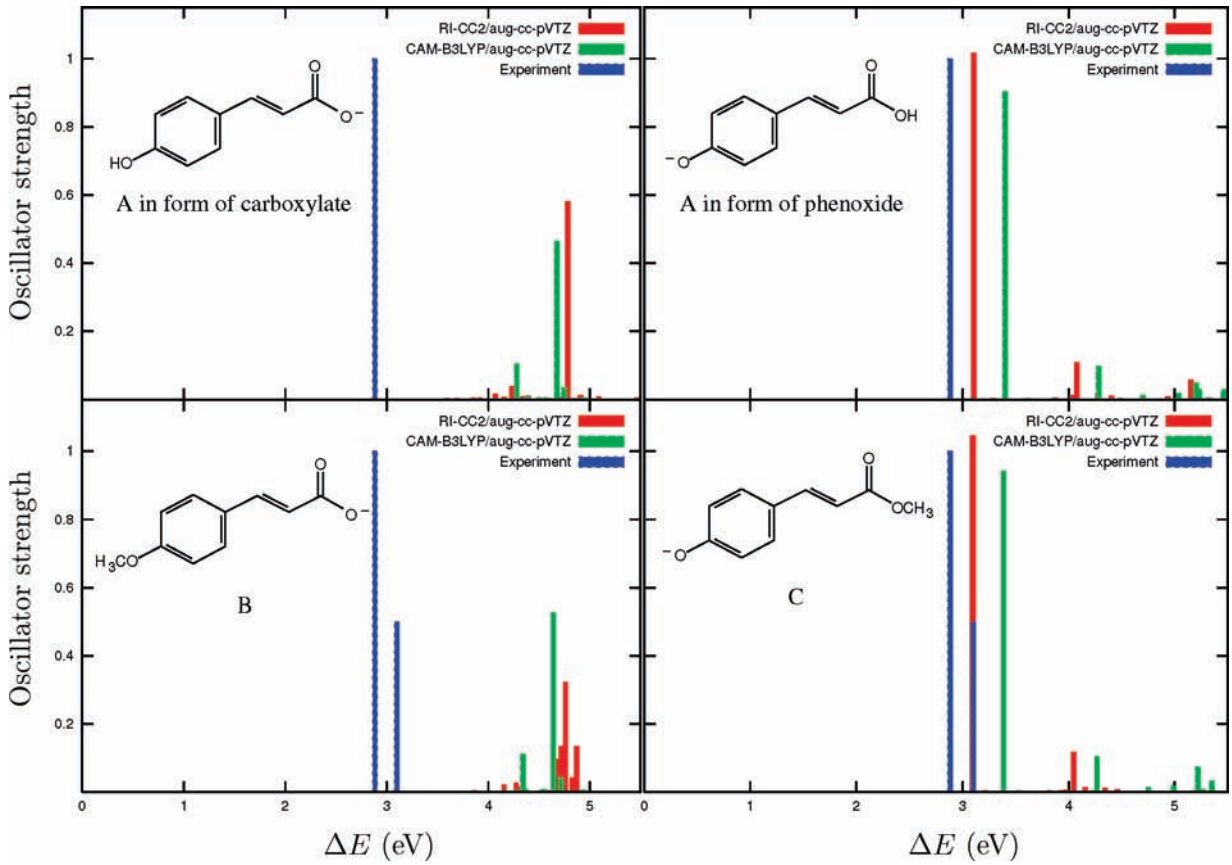

Figure 6. Oscillator strengths calculated using RI-CC2 and CAM-B3LYP, as a function of the excitation energies for the carboxylate and phenoxide anions of the *trans p*-coumaric acid and for systems **B** and **C**. The oscillator strengths of the experimental absorptions at 400 and 430 nm were arbitrarily set to 0.5 and 1.0 respectively.

TABLE 1: S_0-S_1 Vertical Excitation Energies in Nanometers and Electronvolts (in Parentheses) of the Deprotonated *trans p*-Coumaric Acid in the Form of Carboxylate and Phenoxide Computed at the CAM-B3LYP, RI-CC2, State-Specific MRMP2 and Multistate MCQDPT2, aug-MCQDPT2 Levels[a]

Method	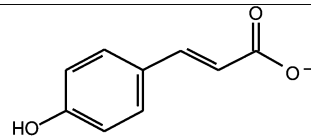	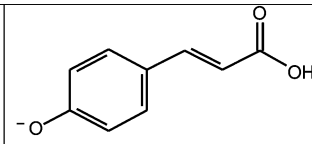
CAM-B3LYP	264 (4.70)	365 (3.40)
RI-CC2	259 (4.79)	400 (3.10)
MRMP2	240 (5.17)	444 (2.79)
MCQDPT2	407 (3.05)	441 (2.81)
aug-MCQDPT2	435 (2.85)	440 (2.82)
Experiment	430 (2.88)	430 (2.88)

[a] The results are shown for the most intensive transitions in the calculations. Experimental data are also presented for comparison.

with the higher-energy excited states, in particular, with one dominated by a double-electron excitation. An improper quality of the CASSCF reference wave function leads to an overestimation of the S_0-S_1 excitation energy by more than 2 eV in the frame of the state-specific MRMP2 approach.

The augmented effective Hamiltonian technique corrects the quality of the target state using a relatively large dimension of the reference space. Within this approximation, the target state is well-separated and admixtures of the higher-energy states are eliminated. This leads to a localization of the wave function in terms of its expansion through configurational state functions. The first improvement was achieved upon the inclusion of six states in the effective Hamiltonian within the smallest reference space which involves the target excited state. This altered dramatically the order of states and lowered the energy of the state of interest (see Table 1). The final value, 435 nm, is very close to the experimental one, 430 nm. The fourth column of Table 2 represents the final results for the S_0-S_1, S_0-S_2, and S_0-S_3 transitions obtained by the augmented multistate MCQDPT2 approximation: the corresponding vertical excitation wavelengths are 435, 360, and 290 nm, respectively. The expansions of the final states through the configurational state functions are different from those corresponding to the MRMP2/CASSCF results of the second column of Table 2, although the transition types determined by the leading configurations remain the same.

TABLE 2: Low-Energy Part of the Spectrum of the Carboxylate Anion of *trans p*-Coumaric Acid Obtained at the Augmented MCQDPT2, MRMP2, and RI-CC2 Levels[a]

transition type	RI-CC2	MRMP2	aug-MCQDPT2
target $\pi-\pi^*$	259 (0.58)	240 (0.59)	435 (0.42)
charge transfer $\pi-\pi^*$	305 (0.02)	344 (0.02)	360 (0.03)
partial charge transfer $\pi-\pi^*$	293 (0.04)	304 (0.04)	290 (0.04)

[a] The strongest computed bands are presented. The excitation energies are in nanometers, while the oscillator strengths are presented in parantheses.

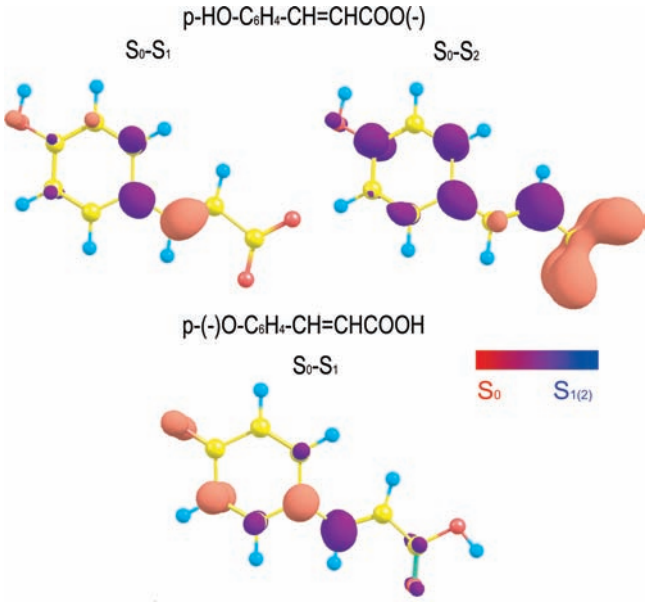

Figure 7. Differential aug-MCQDPT2 electron densities of the first transitions of the carboxylate and phenoxide anions of *trans p*-coumaric acid. Red and blue colors correspond to negative and positive signs respectively of the differential electron density.

The character of the transitions for both isomers of system A can be analyzed in terms of the electron density redistribution upon the excitation obtained as a difference of the excited and ground state aug-MCQDPT2 zero-order densities. The S_0-S_1 and S_0-S_2 differential electron densities of the carboxylate anion of pCA as well as that associated with the S_0-S_1 transition of the phenoxide isomer are shown in Figure 7. The types of the S_0-S_1 transition are similar for both forms of system A with the dominant redistribution occurring in the central part. However, essential differences can be pointed out. The negative charge of the carboxylate group does not participate in the electron density redistribution upon excitation in contrast to the phenoxide system characterized by an electron density transfer from the phenoxy ring to the β carbon and the carboxylic acid group. Furthermore, the electron density transfer occurs in different directions along the molecule as it can be expected taking into account the distribution of the negative charge in both anions. Therefore, the electron density transfer upon excitation causes a significant change in the dipole moment of the phenoxide anion, more concisely $|\Delta\vec{\mu}| = 5$ D. This large change in the dipole moment leads to the higher oscillator strength of the S_0-S_1 transition of the phenoxide form of system A ($f = 0.99$) in comparison with that of the carboxylate ($f = 0.42$). Despite the large change in the dipole moment for the phenoxide form of pCA^-, the aforementioned inefficient solvation of the phenoxide moiety by methanol impairs the solvatochromism of this anion. This is evidenced by the fact that the gas phase absorption

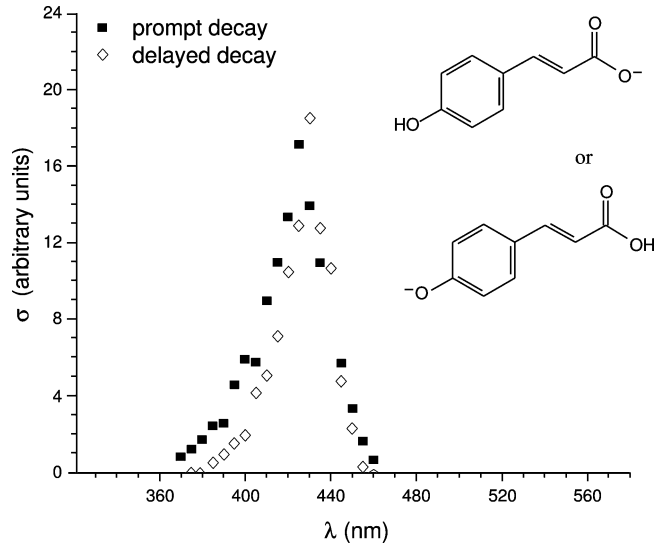

Figure 8. Absorption contribution for the content of the prompt and the delayed decay channels of system **A**.

spectrum of C is less blue-shifted than that of B in CH_3OH (Figure 3 and Figure 5). The S_0-S_2 transition in the carboxylate form of system A, predicted to be the lowest energy excitation by the RI-CC2, CAM-B3LYP, and the state-specific MRMP2, has an enhanced charge transfer character, but it is associated with a very low oscillator strength. Thus, this band is most probably undetectable by the experiment.

Additional calculations of the n-π^* vertical excitation energies at the MRMP2/aug-cc-pVTZ level revealed that these transitions fall within the same range as the target $\pi-\pi^*$ energy excitation in system B. In particular, the estimated value for the vertical excitation energy is 377 nm, which is quite close to the experimental spectral feature observed at the wavelength just below 400 nm. Furthermore, the RI-CC2 method also gives a similar value, 374 nm, which can be assigned to a n-π^* transition. Usually, the oscillator strength of this type of excitation is negligible unless the low energy vibrations of the carboxylate group contribute to intensify the transitions.

Photoresponse Channels. The photoabsorption signal recorded for the model chromophores is categorized as prompt and delayed based on the time at which it appears after laser excitation. If there are statistical decay channels that occur in the first few microseconds after the excitation, they can contribute only to the prompt signal and not to the delayed one. The yield of photofragments as a function of wavelength for both the prompt and the delayed mode of decay is depicted in Figure 8 for system A. Since both decay modes have the same absorption profile, it is concluded that both address the same excited state of the chromophore. A significant prompt signal was observed in all of the three systems, A, B, and C, but the delayed statistically decaying mode was observed only for sample A.

All of the three systems show fragmentation after photoexcitation as an active mode of decay. A daughter mass fragment of 146 ± 2 amu was recorded for samples B and C. The presence of a daughter mass of 119 ± 2 for system A was reported recently.[20] The neutral fragments were determined to be OCH_3 from the daughter-mass analysis at ELISA in both cases. The possible dissociation pathways for the three chromophores are depicted in Figure 9.

The TOF spectra of the neutral fragments from systems B and C under the influence of an electric field are shown in Figure

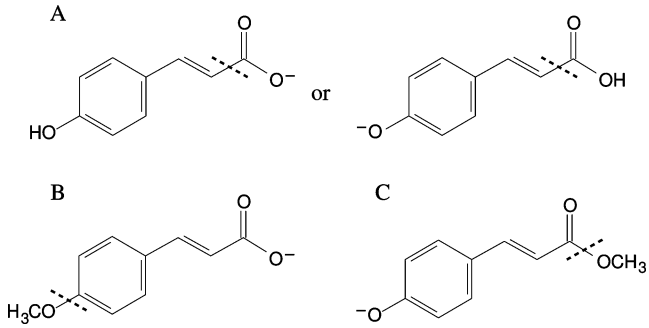

Figure 9. Possible dissociative decay channels for systems **A**, **B**, and **C**.

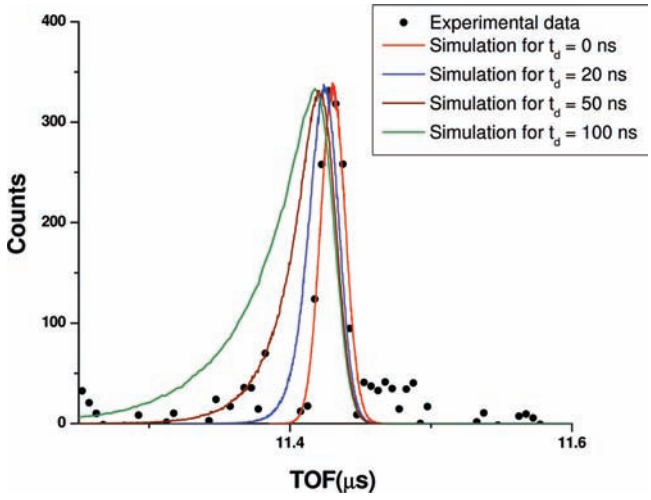

Figure 10. Experimental time-of-flight spectra recorded with $V_{spec} = -2.5$ kV for system **B** along with Monte Carlo simulations for the dissociation lifetimes $t_D = 0$, 20, 50, and 100 ns.

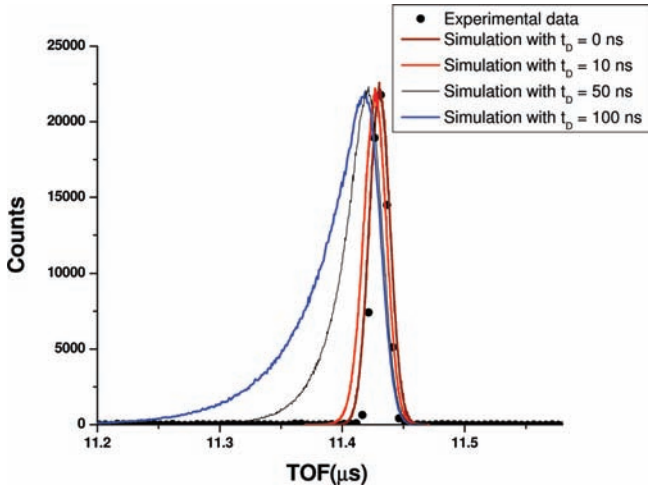

Figure 11. Experimental time-of-flight spectra recorded with $V_{spec} = -2.5$ kV for system **C** along with Monte Carlo simulations for the dissociation lifetimes $t_D = 0$, 10, 50, and 100 ns.

10 and in Figure 11. Neither of the methylated systems yielded a peak corresponding to dissociations occurring outside the electric field region, emphasizing the fast nature of the neutral fragment formation. Monte Carlo simulations were performed for the TOF of the neutral fragments to deduce an upper limit of the dissociation lifetime, and they are shown in Figure 10 and in Figure 11. The results indicate that the dissociation is faster than 20 and 10 ns for systems B and C respectively.

No detachment signal of photoelectrons was observed for system B at 400 nm (3.1 eV) in agreement with the fact that the electron detachment energy of a carboxylate moiety is known to be close to 3.5 eV.[44] On the other hand, photoelectrons were detected for system C like Lee et al.[7] did in a similar anion bearing the phenoxide functional group. Thus, the observed fast pathways of relaxation of system C have contributions from both detachment and dissociation. Electron detachment was previously observed as a photoresponse channel for pCA^- as well.[20] This indicates that there was a detectable amount of the phenoxide isomer in system A in concordance with our calculations which suggest that this isomer is more stable than the carboxylate form in gas phase. Because every system presented fragmentation as a photodissociation pathway, we cannot ascertain whether the ion bunch of pCA^- contained the carboxylate isomer in addition to the phenoxide anion.

The electron detachment threshold from either a π-orbital or an *n*-orbital of system B is equal to 365 and 301 nm, respectively, at the MRMP2 approximation. The calculated vertical-ionization potential at the RI-CC2 level is 292 nm. Therefore, the autoionization threshold from a π orbital is very close to the energies of the bound n-π^* transitions. It is worth noting that the geometry of the neutral radical system is close to that of the anion. The largest deviations are related to the geometry of the carboxylate moiety. The $C-COO^-$ bond is increased and the $O-C-O$ angle is reduced in the neutral radical species with reference to the corresponding values in the anion. Importantly, the ionization potential depends strongly on the geometry, causing the vibrations of the carboxylate to have a great impact on the ionization energies. The vertical ionization potential calculated with the equilibrium geometry of the neutral radical species is considerably red-shifted with respect to that determined using the equilibrium geometry of the anion. Hence, our calculations suggest that the electron emission may be an important mode of relaxation along with the photodissociation decay channel after photoexcitation in the gas phase.

Concluding Remarks

The photoactive yellow protein chromophore model, *trans p*-coumaric acid, has two acidic protons, and therefore, the gas phase structure of its deprotonated form produced by the electrospray technique can correspond to either a phenoxide or a carboxylate. In addition, the deprotonation site of the *trans p*-coumaric acid is expected to have an influence on its absorption spectrum. The pK_a values of the chromophore predict that its deprotonated form has a structure of a carboxylate rather than a phenoxide in solution. RI-CC2 and DFT calculations indicate that the acidity of the phenolic and carboxylic acids is reversed in gas phase. The photoabsorption spectra of the deprotonated *trans p*-coumaric acid and two of its methyl derivatives were measured in order to determine the gas phase structure of the deprotonated *trans p*-coumaric acid and the effect of the deprotonation site in the spectral response. The deprotonated methyl derivatives showed the same absorption maximum as the anion of the *trans p*-coumaric acid in gas phase. However, the deprotonation site is relevant in the absorption spectrum in polar solvents. The methyl derivatives which have a carboxylate or a phenoxide functional group absorb at different wavelengths in alcoholic solution by virtue of their different interactions with the solvent. It was also found that the three studied systems exhibit different fragmentation time scales, although they have the same absorption maximum. A fast decay process (<10 μs) was observed for all three samples while a delayed mode of decay was recorded only for the deprotonated *trans p*-coumaric acid. The analysis of the photodissociation pathways indicated that the phenoxide isomer is present in a

substantial amount in the deprotonated *trans p*-coumaric acid in gas phase while the occurrence of the caboxylate form could not be ascertained. The single-reference ground state linear response methods as well as the multireference perturbative approaches agree with experiment in the description of the phenoxide systems, but only aug-MCQDPT2 agrees with experiment in the description of the carboxylates. The discrepancy of RI-CC2 relative to experiment for the carboxylate anions is against all previous experience as the basic conditions for the successful use of this method seem fulfilled. While the measurements themselves seem very conclusive, the possibility of other interpretations may be considered. However, all our checks only led to support that, during the recording of system B, we are dealing with the photoabsorption of the carboxylate anion. The difficulty in the description of the low-energy region of the absorption spectra of the carboxylate systems is a puzzle that should attract further theoretical investigations.

Acknowledgment. This work was supported by the Lundbeck, Carlsberg, and Willum Kann Rasmussen Foundations, the Danish Research Agency (Contract No. 272-06-0427) and by the grant from the Russian Foundation for Basic Research (Project No. 08-03-00914-a). O.C. acknowledges support from the Danish Center for Scientific Computing (DCSC), the Danish national research foundation and EUROHORCs for a EURYI award. The authors gratefully acknowledge Professor T. Helgaker and Professor P. Salek for providing them with a CAM-B3LYP implementation in Dalton prior to general release and Professor L. Jullien for support.

Supporting Information Available: Experimental setup for the measurement of the gas-phase absorption spectra and the TOF spectra, computational details about the computation of the vertical excitation energies, and the ionization potential thresholds from n and π orbitals. This material is available free of charge via the Internet at http://pubs.acs.org.

References and Notes

(1) Madigan, M. T.; Martinko, J. M.; Dunlap, P. V.; Clark, D. P. *Brock Biology of Microorganisms*, 12th ed.; Benjamin Cummings, 2008.
(2) *Photomovement*; Ḧader, D.-P., Lebert, M., Eds.; Comprehensive Series in Photoscience; Elsevier: New York, 2001.
(3) Larsen, D. S.; van Grondelle, R. *ChemPhysChem* **2005**, *6*, 828.
(4) Hellingwerf, K. J.; Hendriks, J.; Gensch, T. *J. Phys. Chem. A* **2003**, *107*, 1082.
(5) van der Horst, M. A.; Hellingwerf, K. J. *Acc. Chem. Res.* **2004**, *37*, 13.
(6) Ryan, W. L.; Gordon, D. J.; Levy, D. H. *J. Am. Chem. Soc.* **2002**, *124*, 6194.
(7) Lee, I.-R.; Lee, W.; Zewail, A. H. *Proc. Nat. Acad. Sci. U.S.A.* **2006**, *103*, 258.
(8) Anderson, S.; Crosson, S.; Moffat, K. *Acta Crystallogr., Sect D: Biol. Crystallogr.* **2004**, *60*, 1008.
(9) Unno, M.; Kumauchi, M.; Sasaki, J.; Tokunaga, F.; Yamauchi, S. *J. Am. Chem. Soc.* **2000**, *122*, 4233.
(10) Groot, M.-L.; van Wilderen, L. J. G. W.; Larsen, D. S.; van der Horst, M. A.; van Stokkum, I. H. M.; Hellingwerf, K. J.; van Grondelle, R. *Biochemistry* **2003**, *42*, 10054.
(11) Molina, V.; Merchán, M. *Proc. Natl. Acad. Sci. U.S.A.* **2001**, *98*, 4299.
(12) Gromov, E. V.; Burghardt, I.; Köppel, H.; Cerderbaum, L. S. *J. Am. Chem. Soc.* **2007**, *129*, 6798.
(13) Gromov, E. V.; Burghardt, I.; Köppel, H.; Cerderbaum, L. S. *J. Phys. Chem. A* **2005**, *109*, 4623.
(14) Gromov, E. V.; Burghardt, I.; Hynes, J. T.; Köppel, H.; Cerderbaum, L. S. *J. Photochem. Photobiol. A* **2007**, *190*, 241.
(15) Sergi, A.; Grüning, M.; Ferrario, M.; Buda, F. *J. Phys. Chem. B* **2001**, *105*, 4386.
(16) Vreede, J.; Crielaard, W.; Hellingwerf, K. J.; Bolhius, P. G. *Biophys. J.* **2005**, *88*, 3525.
(17) Genick, U. K.; Soltis, S. M.; Kuhn, P.; Canestrelli, I. L.; Getzoff, E. D. *Nature* **1998**, *392*, 206.
(18) Nielsen, I. B.; Boyé-Péronne, S.; Ghazaly, M. O. A. E.; Kristensen, M. B.; Nielsen, S. B.; Andersen, L. H. *Biophys. J.* **2005**, *89*, 2597.
(19) Thian, Z.; Kass, S. R. *J. Am. Chem. Soc.* **2008**, *130*, 10842.
(20) Lammich, L.; Rajput, J.; Andersen, L. H. *Phys. Rev. E* **2008**, *78*, 051916.
(21) Karthikeyan, S.; Ramamurthy, V. *J. Org. Chem.* **2007**, *72*, 452.
(22) Møller, S. P. *Nucl. Instrum. Methods Phys. Res., Sect. A* **1997**, *394*, 281.
(23) Støchkel, K.; Kadhane, U.; Andersen, J. U.; Holm, A. I. S.; Hvelplund, P.; Kirketerp, M.-B. S.; Larsen, M. K.; Lykkegaard, M. K.; Nielsen, S. B.; Panja, S.; Zettergren, H. *Rev. Sci. Instrum.* **2008**, *79*, 023107.
(24) Pedersen, H. B.; Jensen, M. J.; Safvan, C. P.; Urbain, X.; Andersen, L. H. *Rev. Sci. Instrum.* **1999**, *70*, 3289.
(25) Lammich, L.; Nielsen, I. B.; Sand, H.; Svendsen, A.; Andersen, L. H. *J. Phys. Chem. A* **2007**, *111*, 4567.
(26) Becke, A. D. *J. Chem. Phys.* **1993**, *98*, 5648.
(27) Stephens, P. J.; Devlin, F. J.; Chabalowski, C. F.; Frisch, M. J. *J. Phys. Chem.* **1994**, *98*, 11623.
(28) Adamo, C.; Barone, V. *J. Chem. Phys.* **1999**, *110*, 6158.
(29) Dunning, T. H. *J. Chem. Phys.* **1989**, *90*, 1007.
(30) Kendall, R. A.; Dunning, T. H.; Harrison, R. J. *J. Chem. Phys.* **1992**, *96*, 6796.
(31) Christiansen, O.; Koch, H.; Jørgensen, P. *Chem. Phys. Lett.* **1995**, *243*, 409.
(32) Hättig, C.; Weigend, F. *J. Chem. Phys.* **2000**, *113*, 5154.
(33) Hättig, C.; Köhn, A. *J. Chem. Phys.* **2002**, *117*, 6939.
(34) Yanai, T.; Tew, D. P.; Handy, N. C. *Chem. Phys. Lett.* **2004**, *393*, 51.
(35) Roos, B. O. *Adv. Chem. Phys.* **1987**, *69*, 339.
(36) Hirao, K. *Chem. Phys. Lett.* **1992**, *190*, 374.
(37) Nakano, H. *J. Chem. Phys.* **1993**, *99*, 7983.
(38) Bravaya, K. B.; Bochenkova, A. V.; Granovsky, A. A.; Nemukhin, A. V. *J. Am. Chem. Soc.* **2007**, *129*, 13035.
(39) Beltrán, J. L.; Sanli, N.; Fonrodona, G.; Barrón, D.; Özkan, G.; Barbosa, J. *Anal. Chim. Acta* **2003**, *484*, 253.
(40) Albert, A.; Serjeant, E. P. *Ionization constants of acids and bases*; John Wiley and Sons, Inc.: New York, 1962; and references therein.
(41) Joly, L.; Antoine, R.; Allouche, A.-R.; Broyer, M.; Lemoine, J.; Dugourd, P. *J. Am. Chem. Soc.*
(42) Meyer, E. A.; Castellano, R. K.; Diederich, F. *Angew. Chem., Int. Ed.* **2003**, *42*, 1210.
(43) Carey, F. A. *Organic Chemistry*, 5th ed.; McGraw-Hill: New York, 2002.
(44) Kim, E. H.; Bradforth, S. E.; Arnold, D. W.; Metz, R. B.; Neumark, D. M. *J. Chem. Phys.* **1995**, *103*, 7801.

JP904660W